Collective Dissipative Molecule Formation in a Cavity

David Wellnitz,[1,2] Stefan Schütz,[1,2] Shannon Whitlock,[1] Johannes Schachenmayer,[1,2,*] and Guido Pupillo[1,3,†]
[1]ISIS (UMR 7006) and icFRC, University of Strasbourg and CNRS, 67000 Strasbourg, France
[2]IPCMS (UMR 7504), University of Strasbourg and CNRS, 67000 Strasbourg, France
[3]Institut Universitaire de France (IUF), 75000 Paris, France

(Received 14 February 2020; accepted 24 September 2020; published 2 November 2020)

We propose a mechanism to realize high-yield molecular formation from ultracold atoms. Atom pairs are continuously excited by a laser, and a collective decay into the molecular ground state is induced by a coupling to a lossy cavity mode. Using a combination of analytical and numerical techniques, we demonstrate that the molecular yield can be improved by simply increasing the number of atoms, and can overcome efficiencies of state-of-the-art association schemes. We discuss realistic experimental setups for diatomic polar and nonpolar molecules, opening up collective light matter interactions as a tool for quantum state engineering, enhanced molecule formation, collective dynamics, and cavity mediated chemistry.

DOI: 10.1103/PhysRevLett.125.193201

There is considerable interest in preparing and manipulating ultracold ensembles of molecules for quantum simulations, metrology, and the study of chemical reactions in the ultracold regime [1–5]. Diatomic molecules in their electronic and rovibrational ground state are routinely produced using the coherent stimulated Raman adiabatic passage (STIRAP) technique [6–10]. Alternatively, continuous formation of ground state molecules can be realized by photoassociation via a weakly bound excited molecular state [11–16]. While more sophisticated methods such as photoassociation followed by pulsed population transfer [17] or repumping of vibrationally excited molecules [18,19] have been experimentally demonstrated, efficiencies of ground state molecular formation are usually lower than those achieved with STIRAP and without rotational state selectivity. It has recently been proposed that these efficiencies can be increased by strengthening light-molecule coupling rates to ground-state transitions using a cavity [20] or a photonic waveguide [21]. Common to all these schemes is the use of formation processes based on single molecules.

Here, we propose a mechanism to exploit collective effects to perform continuous high-yield molecular formation from ultracold atoms in a cavity. Our scheme is based on photoassociation to a collective excited bound state followed by superradiant-type decay induced by the cavity to the molecular ground state. We consider the regime of large dissipation with negligible number of cavity photons and electronic excitations, and derive an effective master equation for the internal dynamics of N atom pairs. We show that (i) a continuous laser gives rise to enhancement of the fraction of ground state molecules $N_g^\infty/N \sim [1 - \log(N)/(NC)]$ approaching 1, with NC the collective cooperativity; and (ii) a chirped laser pulse that matches the time-varying excited molecular polariton energies can lead to a final molecular yield $N_g^\infty/N \sim 1 - \Gamma/\kappa$, with Γ the excited state linewidth and κ the cavity linewidth. The two schemes are most useful for weak and strong cavity couplings, respectively, for which we provide concrete examples. With scheme (i) collective effects always increase the molecular yields at the cost of decreased transfer rates. In contrast, scheme (ii) cannot be directly compared to the single particle scenario with a cavity, but always has higher yields than single-particle photoassociation without a cavity. Both schemes can serve as alternatives to STIRAP that relax the requirement for expensive, narrow linewidth, phase-coherent lasers [22], and offer a natural way to continuously populate a molecular lattice coupled to a cavity. More broadly, this work exemplifies the opportunities for state engineering using collective effects in the presence of strong dissipation.

We consider a setup consisting of N identical pairs of atoms and a single mode cavity. The external dynamics of each pair is assumed to be frozen, e.g., by confining to an optical lattice potential. We model each atom pair as a four-level system with states $|i\rangle_n, |e\rangle_n, |g\rangle_n$, and $|x\rangle_n$, $1 \le n \le N$. The first three states correspond to a two-atom initial state (e.g., a low-energy scattering state or preformed Feshbach molecular bound state), a molecular excited state, and the absolute electronic and rovibrational molecular ground state, respectively [see Fig. 1(b)]. The fourth level $|x\rangle_n$ represents a set of arbitrary excited molecular (e.g., vibrationally or rotationally excited) or free particle states, whose population we want to avoid. The dynamics of the system's density matrix $\hat{\rho}$ is governed by the master equation $\partial_t\hat{\rho} = -\mathrm{i}[\hat{H}, \hat{\rho}] + \mathcal{D}\hat{\rho}$, with $\hat{H} = \hat{H}_{LA} + \hat{H}_C + \hat{H}_0$ the system Hamiltonian and ($\hbar = 1$)

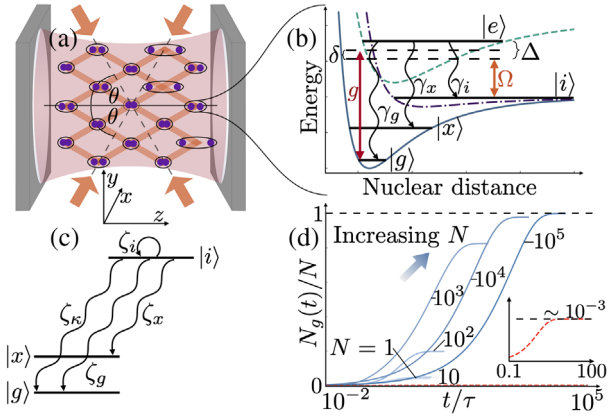

FIG. 1. Basic setup for collective dissipative molecule formation. (a) Feshbach molecules are trapped in a lattice inside a cavity and brought into deeply bound states by photoassociation. An angle θ between the lattice laser beams and the cavity (z) axis ensures mode matching. (b) Scheme of energy levels and their coupling for a single molecule. For RbCs the potential energy curves can be identified with the ground state potential $X^1\Sigma^+$ (continuous line; dissociates to $5s + 6s$), triplet ground state potential $a^3\Sigma^+$ (dash-dotted line; dissociates to $5s + 6s$) and excited state potential $(A^1\Sigma^+ - b^3\Pi)0^+$ (dashed line; dissociates to $5s + 6p$). A molecule prepared in a Feshbach state $|i\rangle$ is laser excited (coupling strength Ω, detuning Δ) into the excited state $|e\rangle$, which can decay back into $|i\rangle$, the rovibrational ground state $|g\rangle$ or any other state (bound or not), here collectively called $|x\rangle$. (c) Energy levels of a single molecule after adiabatic elimination of the cavity and excited state with decay rates ζ_α ($\alpha = \kappa, i, x, g$). (d) Evolution of the target ground state molecular fraction N_g/N as a function of rescaled time t (see text), for different $1 \leq N \leq 10^5$ (log scale). The red dashed line in the inset indicates the results without cavity.

$$\hat{H}_{\mathrm{LA}} = \Omega\sqrt{N}(\hat{S}_{ie} + \hat{S}_{ei}), \tag{1}$$

$$\hat{H}_C = g\sqrt{N}(\hat{a}^\dagger \hat{S}_{ge} + \hat{S}_{eg}\hat{a}). \tag{2}$$

Here, $\hat{H}_{\mathrm{LA}}$ and $\hat{H}_C$ represent the coupling of the transition dipole moments of the transitions $|i\rangle_n \leftrightarrow |e\rangle_n$ and $|e\rangle_n \leftrightarrow |g\rangle_n$ to the laser and cavity fields with Rabi frequency Ω and vacuum Rabi frequency g, respectively. $\hat{S}_{\alpha\beta} = \sum_n \hat{\sigma}^{(n)}_{\alpha\beta}/\sqrt{N}$ are collective operators that couple the internal states of each pair n via $\hat{\sigma}^{(n)}_{\alpha,\beta} = |\alpha\rangle\langle\beta|_n$ ($\alpha, \beta = i, e, g, x$). $\hat{H}$ is defined in a rotating frame [23] with the detunings of the laser and the cavity, $\Delta = \omega_{ie} - \omega_L$ and $\delta = \omega_C - \omega_L - \omega_{gi}$, respectively. These are included in $\hat{H}_0 = \Delta\hat{N}_e + \delta\hat{a}^\dagger\hat{a}$, where $\hat{N}_\alpha = \sum_n \hat{\sigma}^{(n)}_{\alpha\alpha}$ are total state populations, $\hat{a}$ is the cavity photon annihilation operator, and ω_L, ω_C, and $\omega_{\alpha\beta}$ are the frequencies of the laser, the cavity, and the transitions, respectively.

Dissipative terms are described by the superoperator

$$\mathcal{D}\hat{\rho} = \mathcal{L}[\hat{L}_\kappa]\hat{\rho} + \sum_{n=1}^{N}(\mathcal{L}[\hat{L}^{(n)}_{\gamma_i}] + \mathcal{L}[\hat{L}^{(n)}_{\gamma_x}] + \mathcal{L}[\hat{L}^{(n)}_{\gamma_g}])\hat{\rho}, \tag{3}$$

with $3N + 1$ decay channels, each governed by a Lindblad term $\mathcal{L}[\hat{L}]\hat{\rho} = -\{\hat{L}^\dagger\hat{L}, \hat{\rho}\} + 2\hat{L}\,\hat{\rho}\,\hat{L}^\dagger$. Here we include cavity decay with rate 2κ, $\hat{L}_\kappa = \sqrt{\kappa}\hat{a}$, and spontaneous emission from the excited state $|e\rangle_n$ for each pair n, $\hat{L}^{(n)}_{\gamma_\alpha} = \sqrt{\gamma_\alpha}\hat{\sigma}^{(n)}_{\alpha e}$ with rates $2\gamma_\alpha$ for $\alpha = i, g, x$. We define $\Gamma = \sum_\alpha \gamma_\alpha$ and the complex detunings $\tilde{\Delta} = \Delta - i\Gamma$ and $\tilde{\delta} = \delta - i\kappa$.

In the regime of strong dissipation, both the excited states and the cavity mode are weakly populated $\langle \hat{N}_e + \hat{a}^\dagger\hat{a}\rangle \ll 1$ and can be adiabatically eliminated [23,31]. Then, the dynamics reduces to an effective master equation for the sub-systems $\{|i\rangle_n, |g\rangle_n, |x\rangle_n\}$ [see Fig. 1(c)]. We find that the new effective Lindblad operators read

$$\hat{L}^{\kappa}_{\mathrm{eff}} = \sqrt{\lambda_\kappa}\hat{\xi}\hat{S}_{gi} \qquad \hat{L}^{\alpha,(n)}_{\mathrm{eff}} = \sqrt{\lambda^\alpha_\gamma}(\hat{\sigma}^{(n)}_{\alpha i} - \hat{\sigma}^{(n)}_{\alpha g}\hat{\xi}\hat{S}_{gi}). \tag{4}$$

The terms $\hat{L}^{\kappa}_{\mathrm{eff}}$ and $\hat{L}^{\alpha,(n)}_{\mathrm{eff}}$ in Eq. (4) result from a virtual excitation of the states $|e\rangle_n$ being lost via the cavity or via spontaneous emission, respectively. Here, $\lambda_\kappa = \Omega^2\kappa/g^2$ and $\lambda^\alpha_\gamma = \Omega^2\gamma_\alpha/\tilde{\Delta}^2$ are the respective rates, while $\hat{\xi} = \sqrt{N}g^2(\hat{N}_g g^2 - \tilde{\Delta}\,\tilde{\delta})^{-1}$ is a collective dimensionless operator stemming from the excited state propagator, which captures the effects of virtually excited superradiant states [in the weak light-matter coupling regime $(N_g + 1)g^2 < (\kappa - \Gamma)^2/4$] or virtually excited polaritons [in the strong coupling regime $(N_g + 1)g^2 > (\kappa - \Gamma)^2/4$]. Thus, Eq. (4) gives rise to collective, dissipative, and unidirectional population transfer from the states $|i\rangle_n$ to the desired molecular bound states $|g\rangle_n$ and the loss states $|x\rangle_n$ [see Fig. 1(c)], with rates that depend on the many-body state via $\hat{\xi}\hat{S}_{gi}$.

We find a new effective Hamiltonian

$$\hat{H}_{\mathrm{eff}} = -\frac{\Omega^2}{2\tilde{\Delta}}(\hat{N}_i + \sqrt{N}\hat{S}_{ig}\hat{\xi}\hat{S}_{gi}) + \mathrm{H.c.} \tag{5}$$

The first term $-\Omega^2\hat{N}_i/(2\tilde{\Delta})$ in Eq. (5) corresponds to the usual ac Stark shift for a small coupling Ω. The second term corresponds to the self energy due to a molecule being virtually excited by the laser and exchanging this excitation with the cavity. Since $[\hat{N}_\alpha, \hat{H}_{\mathrm{eff}}] = 0$, $\hat{H}_{\mathrm{eff}}$ cannot drive any coherent population transfer and thus we find that all interesting dynamics is driven by dissipation. In the following, we simulate the effective equations of motion first on bare resonance $\Delta = \delta = 0$, then on resonance with a (virtual) polariton.

Numerically, the master equation evolution with terms from Eqs. (4) and (5) can be efficiently simulated by exploiting the permutation symmetry among the N three level systems, which allows for utilizing a collective spin basis [32]. In practice we furthermore employ a quantum trajectory method [23,32,33]. In the numerical simulations, the initial state is the product $\bigotimes_n |i\rangle_n$.

For $\Delta = 0$, we choose typical parameters for RbCs as measured in Ref. [34] [see also Fig. 1(b) and Ref. [23]]. We consider up to $N = 10^5$ molecules trapped in a three-dimensional optical lattice created by a laser with wavelength $\lambda_{\mathrm{latt}} = 1064.5$ nm. Two lattice beams are placed at angles $\pm\theta$ ($\theta = \arccos[\lambda_{\mathrm{latt}}/(2\lambda_{\mathrm{eg}})] = 57°$) with respect to the cavity axis in order to match a desired cavity mode [Fig. 1(a) and below]. The excited state has a half linewidth $\Gamma/2\pi = 2.65$ MHz. The branching ratios $f_\alpha \equiv \gamma_\alpha/\Gamma$ for the decay from $|e\rangle$ into the states $|x\rangle$, $|g\rangle$, and $|i\rangle$ are $f_x \approx 0.999$, $f_g = 1.3 \times 10^{-3}$, and $f_i = 1.3 \times 10^{-4}$, respectively, such that photoassociation without a cavity leads to a maximal asymptotic value of $(\langle \hat{N}_g \rangle/N)(t \to \infty) \equiv (N_g/N)(t \to \infty) \equiv N_g^\infty/N = f_g/(f_g + f_x) \approx 1.3 \times 10^{-3}$. The photoassociation laser (wavelength of $\lambda_{\mathrm{PA}} = 1557$ nm) has a Rabi frequency $\Omega/2\pi = 70$ kHz in the weak coupling regime. We assume a cavity of length $L = 280$ μm, free spectral range $c/2L = 535$ GHz, mode waist $\omega_0 = 12$ μm, and half linewidth $\kappa/2\pi = 5.4$ MHz, which is tuned in resonance with the $\lambda_{\mathrm{eg}} = 977$ nm transition $|e\rangle \leftrightarrow |g\rangle$, resulting in a peak vacuum Rabi frequency $g/2\pi = d_{\mathrm{el}}\sqrt{f_g \omega_{ge}/2\hbar\varepsilon_0 V}/2\pi = 770$ kHz with the mode volume $V = \pi\omega_0^2 L/4$ and the electronic transition dipole moment $d_{\mathrm{el}} = 0.1$ a.u. [34]. We assume the temperature to be small enough so that all molecules are in the lowest lattice band. For a typical lattice depth of $E_0 = 48E_R$ [7], with $E_R = (2\pi\hbar/\lambda_{\mathrm{latt}})^2/(2m_{\mathrm{RbCs}})$ the recoil energy, this implies $T \ll 400$ nK, but even for higher temperatures the scheme may be beneficial [23].

For $\Delta = \delta = 0$, we find $\hat{H}_{\mathrm{eff}} = 0$ and the dynamics is governed by dissipative Lindblad terms *only*, with $\hat{\xi} = \sqrt{N}C(1 + \hat{N}_g C)^{-1}$. Figure 1(d) shows exemplary results for the time evolution of the molecular ground state fraction N_g/N as a function of N, with $1 \le N \le 10^5$ in units of the characteristic time scale $\tau = \Gamma\Omega^{-2}$. For $N = 1$ the figure shows that the presence of a cavity (here $C \approx 0.04$) induces an enhancement of N_g^∞/N from $\sim$0.1% (no cavity, dashed red line) to $\sim$4%, due to increased state selectivity [20]. Strikingly, with increasing N, we observe an enhancement towards $N_g^\infty/N \to 1$, at the cost of an increased transfer time. Figure 2(a) is a contour plot of the long-time population fraction N_x^∞/N in the loss state $|x\rangle$ as a function of N and C. The plot shows that, for increasing collective cooperativity NC, N_x^∞/N rapidly decreases from its bare (no-cavity) value $\sim$1 towards 0 [upper right corner in Fig. 2(a)].

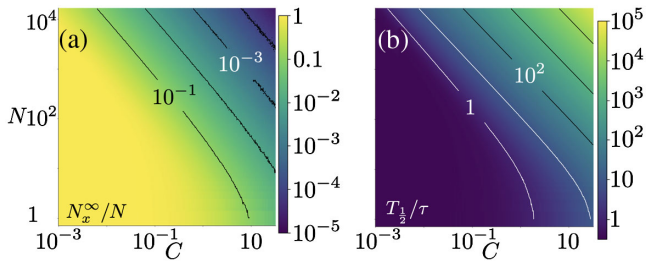

FIG. 2. On bare resonance: (a) Contour plot of the final population fraction in the loss state $|x\rangle$, N_x^∞/N, as a function of the number N of molecules in the cavity and the single molecule cooperativity C. (b) Contour plot of the time $T_{\frac{1}{2}}$ needed to transfer half of the population away from the state $|i\rangle$ in $\tau = \Gamma\Omega^{-2}$. All axes are logarithmic.

To gain further insight, we obtain an analytical solution of the dynamics in the limit of large collective cooperativity $NC \gg 1$ and large but finite ground state molecule number $N_g \gg 1$. In the quantum trajectories picture, the decay rate of a state $|\psi\rangle$ is given by $\langle\psi| - 2\sum \hat{L}_{\mathrm{eff}}^\dagger \hat{L}_{\mathrm{eff}}|\psi\rangle$. With these assumptions, we can restrict the discussion to the symmetric Dicke states, assume $(N_g + 1)C \gg 1$, and neglect fluctuations by approximating operators by their expectation values $N_\alpha \equiv \langle \hat{N}_\alpha \rangle$. We then obtain the following rates for the decays via the different channels [23]

$$2\langle \hat{L}_{\mathrm{eff}}^{\kappa\dagger} \hat{L}_{\mathrm{eff}}^{\kappa} \rangle \approx \frac{2}{\tau}\frac{N_i}{(N_g + 1)C} \equiv \zeta_\kappa, \tag{6}$$

$$2\sum_n \langle \hat{L}_{\mathrm{eff}}^{\alpha,(n)\dagger} \hat{L}_{\mathrm{eff}}^{\alpha,(n)} \rangle \approx \frac{2f_\alpha}{\tau}\frac{N_i}{(N_g + 1)^2 C^2} \equiv \zeta_\alpha. \tag{7}$$

For $(N_g + 1)C \gg 1$, the cavity-decay dominates, $\zeta_\kappa \gg \zeta_\alpha$. Dynamics is then governed by the nonlinear rate equations $\dot{N}_i = -\zeta_x - \zeta_g - \zeta_\kappa$, $\dot{N}_x = \zeta_x$, and $\dot{N}_g = \zeta_g + \zeta_\kappa$, for which we provide analytical solutions in Ref. [23] for the time dependence of the populations, $N_\alpha(t)$. For large N_g^∞, we find for the loss state fraction

$$\frac{N_x^\infty}{N} \approx \frac{f_x \ln(N)}{NC} \overset{NC\to\infty}{\longrightarrow} 0, \tag{8}$$

demonstrating a collective improvement over the single molecule result $f_x/(C + 1)$ of Ref. [20]. The half time $T_{\frac{1}{2}} = \int_{N_i=N}^{N/2} dN_i/\dot{N}_i$ for population transfer out of state $|i\rangle$ is well approximated by

$$T_{\frac{1}{2}} \sim NC\tau. \tag{9}$$

This scaling is observed as straight contours for large NC in the numerical simulations of Fig. 2(b). The demonstration of increased molecular yield in the ground state due to collective dissipative effects, at the cost of decreased transfer rates, is one of the central results of this work.

We find that the slowdown of $T_{\frac{1}{2}}$ in Eq. (9) is due to terms $\propto 1/[(N_g + 1)C]$ in Eqs. (6) and (7), caused by Zeno blocking of the virtually excited superradiant states and detuning from the virtually excited polaritons. The latter usually dominates and is captured by Fig. 3(a), which is a contour plot of $\dot{N}_i$ as a function of N_g and Δ, with $\delta = \Delta$. For $\Delta = 0$, the figure shows that $\dot{N}_i$ decreases rapidly with

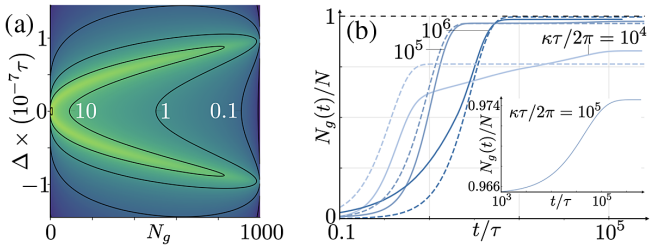

FIG. 3. Chirped pulse: (a) Contour plot of the decay rate of Feshbach molecules $\dot{N}_i$ (in units τ^{-1}, for symmetric Dicke states), as a function of the laser detuning and the number of ground state molecules. The cavity is kept at resonance with the transition energy ($\delta = \Delta$). (b) Simulated time evolution of the ground state population for different cavity decay rates κ. The parameters are chosen for 10^3 Rb_2 molecules inside a cavity [13,20], i.e., $\Gamma/2\pi = 6$ MHz and $g/2\pi \approx 50$ MHz. Dashed lines: analytical fits of Eqs. (13) and (14).

increasing N_g. The rate $\dot{N}_i$ is instead maximized for an optimal choice of detuning,

$$\Delta^{\pm}_{\mathrm{opt}} = \pm\left[\max\left(0, (N_g+1)g^2 - \frac{\Gamma^2+\kappa^2}{2}\right)\right]^{1/2}. \quad (10)$$

This reflects the formation of two polaritons with energy $E^{\pm} \sim \Delta^{\pm}_{\mathrm{opt}}$ for large enough $N_g \gtrsim (\Gamma^2+\kappa^2)/2g^2$. To circumvent the slowdown, we propose to chirp the laser detuning to stay resonant with the polariton energy, which depends on the (time dependent) ground state population $N_g(t)$. This adjustment can be adiabatic since the dynamics of $N_g(t)$ is slow compared to Γ [$\mathcal{O}(\Omega^2/\Gamma)$], and thus it is sufficient to consider a time dependent $\Delta(t)$ and $\delta(t) = \Delta(t)$ in Eqs. (4) and (5).

For $g \ll \kappa + \Gamma \ll \sqrt{N_g+1}g$, the decay rates of the different channels assume the simple form [23,35]

$$2\langle \hat{L}^{\kappa\dagger}_{\mathrm{eff}} \hat{L}^{\kappa}_{\mathrm{eff}} \rangle \approx \frac{2\Omega^2\kappa}{(\kappa+\Gamma)^2} N_i \equiv \zeta_\kappa, \quad (11)$$

$$2\sum_n \langle \hat{L}^{\alpha,(n)\dagger}_{\mathrm{eff}} \hat{L}^{\alpha,(n)}_{\mathrm{eff}} \rangle \approx \frac{2\Omega^2\gamma_\alpha}{(\kappa+\Gamma)^2} N_i \equiv \zeta_\alpha, \quad (12)$$

and the rate equations $\dot{N}_{i,g,x}$ above are solved as

$$\frac{N_i(t)}{N} = \exp\left[-\frac{2\Omega^2(\kappa+\gamma_g+\gamma_x)t}{(\kappa+\Gamma)^2}\right], \quad (13)$$

$$\frac{N_g(t)}{N} = \frac{\kappa+\gamma_g}{\kappa+\gamma_g+\gamma_x}\left\{1 - \exp\left[-\frac{2\Omega^2(\kappa+\gamma_g+\gamma_x)t}{(\kappa+\Gamma)^2}\right]\right\}. \quad (14)$$

These results are formally similar to those of Ref. [21] for a single molecule coupled to a photon waveguide, however, here the cavity decay rate κ is fully tunable. We note that while collective effects are present in the polariton formation, the final rate is independent of N [36]. For $\kappa \gg \gamma_x$, the ground state population approaches N as $N^{\infty}_g/N \simeq 1 - \gamma_x/\kappa$, at the cost of an increasing timescale $\sim\kappa/\Omega^2$, due to the continuous Zeno effect [37].

Figure 3(b) shows a comparison of numerical and analytical results (continuous and dashed lines, respectively) for the increase of N_g/N as a function of time t, for different values of κ. We find good agreement for large values of t/τ and $\kappa\tau$ in the regime of validity of Eqs. (13) and (14), as expected. In addition to this dynamics, a few molecules are trapped in so-called "dark states" $|d\rangle$ that cannot decay via the cavity ($\hat{L}^{\kappa}_{\mathrm{eff}}|d\rangle = 0$). This minor effect is caused by the breaking of permutation symmetry through spontaneous emission [23,38,39], and responsible for a time delay in reaching the asymptotic N^{∞}_g, as magnified in the inset of Fig. 3(b).

Whether higher molecular yields are reached by staying on bare resonance or chirping the laser depends on what limits state selectivity. If transfer times are not a concern, staying on bare resonance is usually best, as we estimate $N^{\infty}_x(\mathrm{chirp}) > N^{\infty}_x(\mathrm{bare})$ for $Ng^2/[\kappa^2 \ln(N)] > 1$ [23]. If instead transfer times are a concern, due, e.g., to background gas collisions, then the chirped scheme may be better, as for a given $T_{\frac{1}{2}}$ we find $N^{\infty}_x(\mathrm{bare}) \sim \ln(N) N^{\infty}_x(\mathrm{chirp})$ [23]. These behaviors, derived for identical cavity coupling strengths g_n, hold also approximately for moderately varying g_n due to, e.g, inhomogeneity of the cavity mode, lattice geometry or thermal motion [23].

For $N = 10^4$ RbCs Feshbach molecules (see parameters above), the system is closer to the first scenario and we find that staying on bare resonance ($\Delta = 0$) provides the highest yield. For a reasonable $1/e$ lattice lifetime of 1 s, we obtain a peak ground state population $N_g/N \approx 92\%$ after 55 ms with a transfer half time $T_{\frac{1}{2}} \approx 3.2$ ms (98% for infinite lattice lifetime). These results are essentially unchanged by considering locally different coupling constants $g_n = g(\mathbf{x}_n) = g\exp[-(x_n^2+y_n^2)/\omega_0^2]\cos(2\pi z_n/\lambda_{\mathrm{eg}})$, due to the finite cavity mode waist ω_0 and the different lattice positions, with z_n (x_n, y_n) oriented along the cavity axis (in the perpendicular planes) [see Fig. 1(a)]. For example, for a $20 \times 20 \times 25$ lattice at angle $\theta = 57°$ and assuming perfect matching of lattice and cavity modes with $\cos(2\pi z_n/\lambda_{\mathrm{eg}}) = 1$ [40], we find a peak $N_g/N \sim 92\%$, a transfer time 48 ms and $T_{\frac{1}{2}} \sim 2.7$ ms, with infinite lattice lifetime final fraction 97%. Thus, ground state populations comparable to STIRAP (~90%) [7,8] can be achieved without the need of time-dependent laser pulses. These results are robust against reasonable lattice mismatches. Even in a worst case scenario of complete positional disorder [i.e., uniform and Gaussian ($\sigma_{xy} = 5$ μm) distributions in the z and $x-y$ directions, respectively] we find a peak $N_g/N \sim 71\%$ (73% for infinite lattice lifetime) after 21 ms and $T_{\frac{1}{2}} \sim 0.4$ ms.

For a scenario with 10^3 Rb_2 Feshbach molecules (see Fig. 3, parameters as in Refs. [13,20]) we are in the regime where the chirped pulse results in a higher yield. For example, choosing a vacuum Rabi frequency $g/2\pi \approx 50$ MHz, a laser Rabi frequency $\Omega/2\pi = 200$ kHz, and a cavity half linewidth $\kappa/2\pi = 300$ MHz, we obtain a ground state population of $N_g/N \approx 98\%$ after 5 ms ($T_{\frac{1}{2}} \sim 0.5$ ms). Even for a spatially disordered worst case scenario (uniform position distribution along z, $\sigma_{xy} = 2.5$ μm, mode waist of 5 μm), we reach a ground state fraction of 89% after 5 ms ($T_{\frac{1}{2}} \sim 0.3$ ms). In both cases this is a significant increase from 54% without cavity, and can overcome typical STIRAP efficiencies [8].

Similar to STIRAP [7,22], the presence of additional excited states in proximity to the $|e\rangle$ state might decrease the transfer efficiency of our schemes. This can be avoided by choosing an excited state with sufficiently large hyperfine and Zeeman splitting [7]. Once the rovibrational ground state is reached, population transfer between the hyperfine sublevels can be achieved with high fidelity [41].

In summary, we proposed two novel methods for high-yield state selective preparation of ultracold molecules in a cavity that exploit collective and dissipative effects. It is an exciting prospect to investigate how similar collective effects could be used to engineer generic state-transfer schemes and even chemical reactions outside of the ultracold regime [42–46], such as room-temperature cavity-modified electron transfer reactions [47,48]. The experimental setups proposed here—molecules trapped on a lattice potential and embedded in a cavity—offer unique opportunities to explore collective dynamics for measurements [49], nonequilibrium quantum phase transitions [50,51], or quantum information applications using long-lived molecular states [52] and cavity-controlled gates [53,54], while also allowing for a nondestructive detection of the molecules [55,56].

We thank Claudiu Genes for helpful discussions. This work is supported by ANR 5 "ERA-NET QuantERA"—Projet "RouTe" (ANR-18-QUAN-0005-01), LabEx ("Nanostructures in Interaction with their Environment," NIE) under contract ANR-11-LABX-0058 NIE within the Investissement d'Avenir program ANR-10-IDEX-0002-02, and IdEx Unistra project STEMQuS. D. W. acknowledges financial support from Agence Nationale de la Recherche (Grant ANR-17-EURE-0024 EUR QMat). G. P. acknowledges support from the Institut Universitaire de France (IUF) and the University of Strasbourg Institute of Advanced Studies (USIAS). Research was carried out using computational resources of the Centre de calcul de l'Université de Strasbourg.

*schachenmayer@unistra.fr
†pupillo@unistra.fr

[1] J. Doyle, B. Friedrich, R. Krems, and F. Masnou-Seeuws, Eur. Phys. J. D **31**, 149 (2004).
[2] L. D. Carr, D. DeMille, R. V. Krems, and J. Ye, New J. Phys. **11**, 055049 (2009).
[3] G. Quemener and P. S. Julienne, Chem. Rev. **112**, 4949 (2012).
[4] S. A. Moses, J. P. Covey, M. T. Miecnikowski, D. S. Jin, and J. Ye, Nat. Phys. **13**, 13 (2017).
[5] J. L. Bohn, A. M. Rey, and J. Ye, Science **357**, 1002 (2017).
[6] J. G. Danzl, M. J. Mark, E. Haller, M. Gustavsson, R. Hart, J. Aldegunde, J. M. Hutson, and H.-C. Nägerl, Nat. Phys. **6**, 265 (2010).
[7] T. Takekoshi, L. Reichsöllner, A. Schindewolf, J. M. Hutson, C. R. Le Sueur, O. Dulieu, F. Ferlaino, R. Grimm, and H.-C. Nägerl, Phys. Rev. Lett. **113**, 205301 (2014).
[8] F. Lang, K. Winkler, C. Strauss, R. Grimm, and J. Hecker Denschlag, Phys. Rev. Lett. **101**, 133005 (2008).
[9] S. A. Moses, J. P. Covey, M. T. Miecnikowski, B. Yan, B. Gadway, J. Ye, and D. S. Jin, Science **350**, 659 (2015).
[10] L. De Marco, G. Valtolina, K. Matsuda, W. G. Tobias, J. P. Covey, and J. Ye, Science **363**, 853 (2019).
[11] K. M. Jones, E. Tiesinga, P. D. Lett, and P. S. Julienne, Rev. Mod. Phys. **78**, 483 (2006).
[12] J. Deiglmayr, A. Grochola, M. Repp, K. Mörtlbauer, C. Glück, J. Lange, O. Dulieu, R. Wester, and M. Weidemüller, Phys. Rev. Lett. **101**, 133004 (2008).
[13] M. A. Bellos, D. Rahmlow, R. Carollo, J. Banerjee, O. Dulieu, A. Gerdes, E. E. Eyler, P. L. Gould, and W. C. Stwalley, Phys. Chem. Chem. Phys. **13**, 18880 (2011).
[14] P. Zabawa, A. Wakim, M. Haruza, and N. P. Bigelow, Phys. Rev. A **84**, 061401(R) (2011).
[15] J. Ulmanis, J. Deiglmayr, M. Repp, R. Wester, and M. Weidemüller, Chem. Rev. **112**, 4890 (2012).
[16] C. D. Bruzewicz, M. Gustavsson, T. Shimasaki, and D. DeMille, New J. Phys. **16**, 023018 (2014).
[17] J. M. Sage, S. Sainis, T. Bergeman, and D. DeMille, Phys. Rev. Lett. **94**, 203001 (2005).
[18] M. Viteau, A. Chotia, M. Allegrini, N. Bouloufa, O. Dulieu, D. Comparat, and P. Pillet, Science **321**, 232 (2008).
[19] H. F. Passagem, R. Colín-Rodríguez, J. Tallant, P. C. Ventura da Silva, N. Bouloufa-Maafa, O. Dulieu, and L. G. Marcassa, Phys. Rev. Lett. **122**, 123401 (2019).
[20] T. Kampschulte and J. Hecker Denschlag, New J. Phys. **20**, 123015 (2018).
[21] J. Perez-Rios, M. E. Kim, and C.-L. Hung, New J. Phys. **19**, 123035 (2017).
[22] N. V. Vitanov, A. A. Rangelov, B. W. Shore, and K. Bergmann, Rev. Mod. Phys. **89**, 015006 (2017).
[23] See Supplemental Material at http://link.aps.org/supplemental/10.1103/PhysRevLett.125.193201 for details on the calculation of the rotating frame, adiabatic elimination, and rate equations, on the implementation of the permutation symmetry, and on the chosen states, and for discussions of the dark states, of different coupling constants, and of finite temperature, which includes Refs. [24–30].
[24] B. A. Chase and J. M. Geremia, Phys. Rev. A **78**, 052101 (2008).
[25] M. Bolaños and P. Barberis-Blostein, J. Phys. A **48**, 445301 (2015).
[26] S. Hartmann, Quantum Inf. Comput. **16**, 1333 (2016).

[27] M. Gegg and M. Richter, New J. Phys. **18**, 043037 (2016).
[28] N. Shammah, S. Ahmed, N. Lambert, S. De Liberato, and F. Nori, Phys. Rev. A **98**, 063815 (2018).
[29] T. Rom, T. Best, O. Mandel, A. Widera, M. Greiner, T. W. Hänsch, and I. Bloch, Phys. Rev. Lett. **93**, 073002 (2004).
[30] J. P. Covey, S. A. Moses, J. Ye, and D. S. Jin, in *Cold Chemistry: Molecular Scattering and Reactivity Near Absolute Zero* (Royal Society of Chemistry, London, 2017), https://doi.org/10.1039/9781782626800-00537.
[31] F. Reiter and A. S. Sørensen, Phys. Rev. A **85**, 032111 (2012).
[32] Y. Zhang, Y.-X. Zhang, and K. Mølmer, New J. Phys. **20**, 112001 (2018).
[33] A. J. Daley, Adv. Phys. **63**, 77 (2014).
[34] M. Debatin, T. Takekoshi, R. Rameshan, L. Reichsöllner, F. Ferlaino, R. Grimm, R. Vexiau, N. Bouloufa, O. Dulieu, and H.-C. Nägerl, Phys. Chem. Chem. Phys. **13**, 18926 (2011).
[35] We note that the inequality $g \ll \kappa + \Gamma$ ensures that staying in resonance with the polariton is possible, as for $g \gtrsim \kappa + \Gamma$ this is prevented by fluctuations of N_g. For small N_g we have $\kappa + \Gamma \gtrsim \sqrt{N_g + 1} g$ and no polariton splitting is present.
[36] This is in contrast to the scheme of Ref. [21], for which collective effects decrease the efficiency due to dark state population caused by individual laser excitations.
[37] C. Gardiner and P. Zoller, *The Quantum World of Ultra-Cold Atoms and Light Book II: The Physics of Quantum-Optical Devices*, Vol. 4 (World Scientific Publishing Company, Singapore, 2015).
[38] N. Shammah, N. Lambert, F. Nori, and S. De Liberato, Phys. Rev. A **96**, 023863 (2017).
[39] M. Gegg, A. Carmele, A. Knorr, and M. Richter, New J. Phys. **20**, 013006 (2018).
[40] Lattice positions are defined as $x_n = (m + 1/2)\lambda_{\mathrm{latt}}/2$, and $y_n = (m' + 1/2)\Delta y$ with $\Delta y = \lambda_{\mathrm{latt}}/[4\sin(\theta)] \approx 317$ nm, with $-10 \leq (m, m') < 10$ integers.
[41] S. Ospelkaus, K.-K. Ni, G. Quéméner, B. Neyenhuis, D. Wang, M. H. G. de Miranda, J. L. Bohn, J. Ye, and D. S. Jin, Phys. Rev. Lett. **104**, 030402 (2010).
[42] J. A. Hutchison, T. Schwartz, C. Genet, E. Devaux, and T. W. Ebbesen, Angew. Chem., Int. Ed. Engl. **51**, 1592 (2012).
[43] A. Thomas, L. Lethuillier-Karl, K. Nagarajan, R. M. A. Vergauwe, J. George, T. Chervy, A. Shalabney, E. Devaux, C. Genet, J. Moran, and T. W. Ebbesen, Science **363**, 615 (2019).
[44] F. Herrera and J. Owrutsky, J. Chem. Phys. **152**, 100902 (2020).
[45] P. Törmä and W. L. Barnes, Rep. Prog. Phys. **78**, 013901 (2015).
[46] T. W. Ebbesen, Acc. Chem. Res. **49**, 2403 (2016).
[47] A. Mandal, T. D. Krauss, and P. Huo, J. Phys. Chem. B **124**, 6321 (2020).
[48] D. Wellnitz, G. Pupillo, and J. Schachenmayer (to be submitted).
[49] A. Niezgoda, J. Chwedenczuk, T. Wasak, and F. Piazza, arXiv:2007.13649.
[50] D. Barberena, R. J. Lewis-Swan, J. K. Thompson, and A. M. Rey, Phys. Rev. A **99**, 053411 (2019).
[51] J. A. Muniz, D. Barberena, R. J. Lewis-Swan, D. J. Young, J. R. K. Cline, A. M. Rey, and J. K. Thompson, Nature (London) **580**, 602 (2020).
[52] P. Rabl, D. DeMille, J. M. Doyle, M. D. Lukin, R. J. Schoelkopf, and P. Zoller, Phys. Rev. Lett. **97**, 033003 (2006).
[53] A. Imamoğlu, D. D. Awschalom, G. Burkard, D. P. DiVincenzo, D. Loss, M. Sherwin, and A. Small, Phys. Rev. Lett. **83**, 4204 (1999).
[54] J. Majer, J. M. Chow, J. M. Gambetta, J. Koch, B. R. Johnson, J. A. Schreier, L. Frunzio, D. I. Schuster, A. A. Houck, A. Wallraff, A. Blais, M. H. Devoret, S. M. Girvin, and R. J. Schoelkopf, Nature (London) **449**, 443 (2007).
[55] R. Sawant, O. Dulieu, and S. A. Rangwala, Phys. Rev. A **97**, 063405 (2018).
[56] M. Zhu, Y.-C. Wei, and C.-L. Hung, Phys. Rev. A **102**, 023716 (2020).